aerospace

MDPI

Article

Comparison of Aerodynamic Loss of a Gas Turbine Vane with Various Trailing Edge Cooling Schemes

Gi-Mun Kim [1], Jin-Young Jeong [2], Young-Jun Kang [2] and Jae-Su Kwak [2,*]

[1] Research Institute for Aerospace Engineering and Technology, Korea Aerospace University, Goyang 10540, Republic of Korea
[2] Department of Aerospace and Mechanical Engineering, Korea Aerospace University, Goyang 10540, Republic of Korea
* Correspondence: jskwak@kau.ac.kr

Abstract: In this study, a comparison of aerodynamic loss of gas turbine vane with various trailing edge configurations was experimentally performed. For the trailing edge, three cooling schemes (the cutback slot, the central injection slot, and the pressure side hole) and three levels of trailing edge diameter (7.5, 10.0, and 12.5% of the throat width, respectively) were considered. The total pressure loss was measured in a five-vane linear cascade at the low-speed mainstream condition (20 m/s) using a Kiel probe and a two-axis traversing device. The measurement region was constrained to the near mid-span region, and the measurement step size was 1 mm. The results showed that the distribution of the total pressure loss was strongly affected by cooling schemes. The vane with the pressure side hole showed a similar distribution to that of the baseline in which a cooling scheme was not applied. It was also shown that the total pressure loss increased as the trailing edge diameter increased regardless of the cooling schemes. Except for the cutback slot cases, there was an inflection point at which the tendency of the area-averaged total pressure loss to the blowing ratio was changed. Through the present study, correlation equations for each cooling scheme were derived against the trailing edge diameter and the blowing ratio.

Keywords: gas turbine; trailing edge cooling; total pressure loss; cutback slot; central injection slot; pressure side hole

Citation: Kim, G.-M.; Jeong, J.-Y.; Kang, Y.-J.; Kwak, J.-S. Comparison of Aerodynamic Loss of a Gas Turbine Vane with Various Trailing Edge Cooling Schemes. *Aerospace* **2023**, *10*, 143. https://doi.org/10.3390/aerospace10020143

Academic Editor: Qiang Zhang

Received: 6 January 2023
Revised: 30 January 2023
Accepted: 2 February 2023
Published: 4 February 2023

1. Introduction

For the higher efficiency of the Brayton cycle-based gas turbine, higher turbine inlet temperatures have typically been preferred. Combustion gas with extremely high temperatures is introduced into the first-stage vanes, so they experience a higher heat load.

Compared with the leading edge and mid-chord region of the vane, the trailing edge is vulnerable to thermal and mechanical stresses due to its relatively thin thickness. A thinner thickness of the trailing edge has a benefit in pressure loss, but a certain thickness is still required for current state-of-the-art turbine vanes (or blades) to accommodate the cooling design elements. Therefore, understanding these conflicting demands on the trailing edge design in terms of cooling and aerodynamic performance is required for gas turbine developers.

Many efforts to understand the physics of aerodynamic loss have been made for decades. Denton [1] provided fundamental insight into the mechanism of loss generation in turbomachinery. He defined the loss in terms of entropy generation due to the viscous effect and divided the total loss into profile loss, endwall loss, and leakage loss, respectively. He also said that profile loss is a major contributor to the total loss. The results of Mee et al. [2] showed that about one-third of the total loss was attributed to the trailing edge loss, which belongs to the profile loss.

Aerodynamic loss of turbine vanes (or blades) is significantly affected by trailing edge shape and thickness. Melzer and Pullan [3] experimentally analyzed the unsteady

mechanism in the trailing edge base region of a transonic turbine blade by performing the Schlieren flow visualization. They investigated the effect of trailing edge shapes (round, square, and elliptical) and reported that the elliptical shape had a benefit in trailing edge loss because it effectively suppresses the transonic vortex shedding. Granovskiy et al. [4] experimentally and numerically investigated a transonic turbine blade in which the trailing edge has discrete cooling holes. They measured aerodynamic losses in a blade cascade with different trailing edge shapes and thicknesses. The results showed that the losses increased as the trailing edge thickness increased regardless of the trailing edge shape. And the blunt trailing edge showed higher loss levels due to flow separation at the sharp corner of the trailing edge. They also found that the higher cooling injection might lead to a decrease in losses due to the momentum addition and the pressure recovery in the base region.

Parra et al. [5] questioned whether the trailing edge loss models derived from the research results of traditional airfoils could be applicable to the airfoil design for the modern highly loaded gas turbine. They carried out flow measurements in the linear vane cascade. In general, thinner trailing edges lead to smaller profile loss; however, their results showed that thicker trailing edges could cause smaller boundary layer loss due to the larger blockage and the increased velocity. This reduction in the boundary layer loss compensates for the enhanced trailing edge loss.

Schobeiri [6] performed theoretical work to find an optimum trailing edge injection at given mass flow ratios. He reported that the minimum mixing losses of the trailing edge were achieved when the velocity ratio between the injected coolant and the mainstream was one. After a decade, Schobeiri and Pappu [7] experimentally compared their experimental results with the theoretical results by Schobeiri [6] and confirmed a good agreement between them.

Various trailing-edge cooling schemes have been introduced in order to reduce the aerodynamic loss of gas turbines. Aminossadati and Mee [8] studied the effect of the span-wise injection angle of the trailing edge central injection slot on the aerodynamic loss by measuring the flow field using a five-hole probe in a linear cascade. The results showed that the injection angle effect became significant at higher mass flow ratio conditions.

Martini et al. [9] performed a comprehensive study on film cooling and heat transfer of the trailing edge with the cutback slot. In a follow-up study, an unsteady detached eddy simulation (DES) was carried out to take a detailed look at the unsteady film mixing process on the cutback surface [10]. They said that unsteady flow phenomena near the lip of the cutback slot affected the mixing process on the cutback surface. Holloway et al. [11] studied the film cooling of the trailing edge with the cutback slot under realistic engine conditions. They analyzed the flow field behind the lip of the cutback slot and reported the momentum of the coolant increased as the blowing ratio increased, which led to an increase in aerodynamic loss.

Uzol et al. [12] investigated the internal fluid mechanic loss of a turbine blade in which the cutback slot was installed and presented the discharge coefficient as a function of the mainstream Reynolds number and geometric features (the cutback length, span-wise rib spacing, and chordwise rib length). They reported that the interaction between the external wall jet and the mainstream strongly affected the losses. Uzol and Camci [13] studied the external aerodynamic losses of a turbine blade in which the cutback slot was installed. They measured the flow field in the near wake zone and the total pressure loss using particle image velocimetry and a pressure probe, respectively. They found that the aerodynamic loss increased as the coolant injection rate increased due to the intensified interaction between the mainstream and the coolant. However, when the coolant injection rate exceeded a certain level, the aerodynamic loss was reduced. And a similar trend of the total pressure loss to the coolant injection rate was reported by Gao et al. [14]. Kapteijn et al. [15] evaluated the aerodynamic performance of a transonic turbine vane with different trailing edge cooling schemes (pressure side ejection and trailing edge ejection). Their results indicated that much faster mixing occurred, and higher loss levels were obtained in the case of the pressure side ejection. Rehder [16] presented a comparison of the

aerodynamic performance of a turbine blade with typically applied trailing edge cooling schemes—the central trailing edge ejection, the pressure side cutback, and the pressure side film holes, respectively. He divided the total aerodynamic loss into individual loss contributors such as shocks, airfoil boundary layers, trailing edge, and mixing process of the coolant and the mainstream. The results showed that the central trailing edge ejection model showed better aerodynamic performance because the injected coolant directly filled the blade wake zone and resulted in aerodynamic loss reduction.

Since the cooling efficiency is different for each coolant scheme, an appropriate cooling scheme should be adopted in consideration of the operating environment and the required cooling efficiency. According to recent studies, it is confirmed that the cutback slot scheme was commonly adopted for the first stage vanes, which experience high thermal load. In addition, most previous studies separately considered the effects of trailing edge shape or cooling scheme on the aerodynamic loss. In this study, the aerodynamic performance of a gas turbine vane in consideration of both trailing edge diameters and various cooling schemes was investigated. As a measure of aerodynamic performance, the total pressure loss coefficient was measured and compared. Correlation equations for each cooling scheme were derived against the trailing edge diameter and the blowing ratio to provide a fundamental database necessary in the initial design stage for the vane airfoil.

2. Experimental Setup

2.1. Vane Airfoil with Different Trailing Edge Diameters

In the present study, the effect of trailing edge thickness on the total pressure loss of the turbine vane was investigated. As shown in Figure 1a, the trailing edge of the tested vane has a conventional circular shape, so the thickness of the trailing edge is varied by considering different trailing edge diameters: 7.5%, 10.0%, and 12.5% of the throat width T, respectively. Although the difference in the trailing edge diameter yields different airfoil layouts, the airfoils were designed to meet the identical throat width between the vanes. Consequently, the mainstream flow rate through the cascade passage was sustained regardless of the trailing edge diameter.

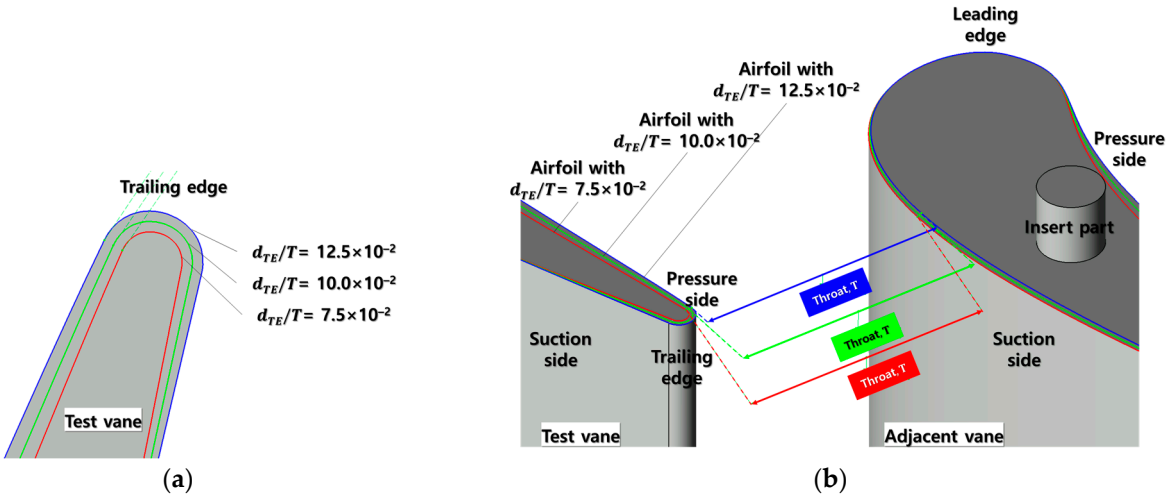

Figure 1. The schematic of the tested vane with different trailing edge diameters: (**a**) airfoil layout showing various trailing edge diameters; (**b**) throat width of vane array.

2.2. Cooling Schemes on the Trailing Edge

Figure 2 shows the schematic of the tested vane trailing edges with various cooling schemes. And a solid trailing edge in which a cooling scheme was not applied was considered as the baseline case.

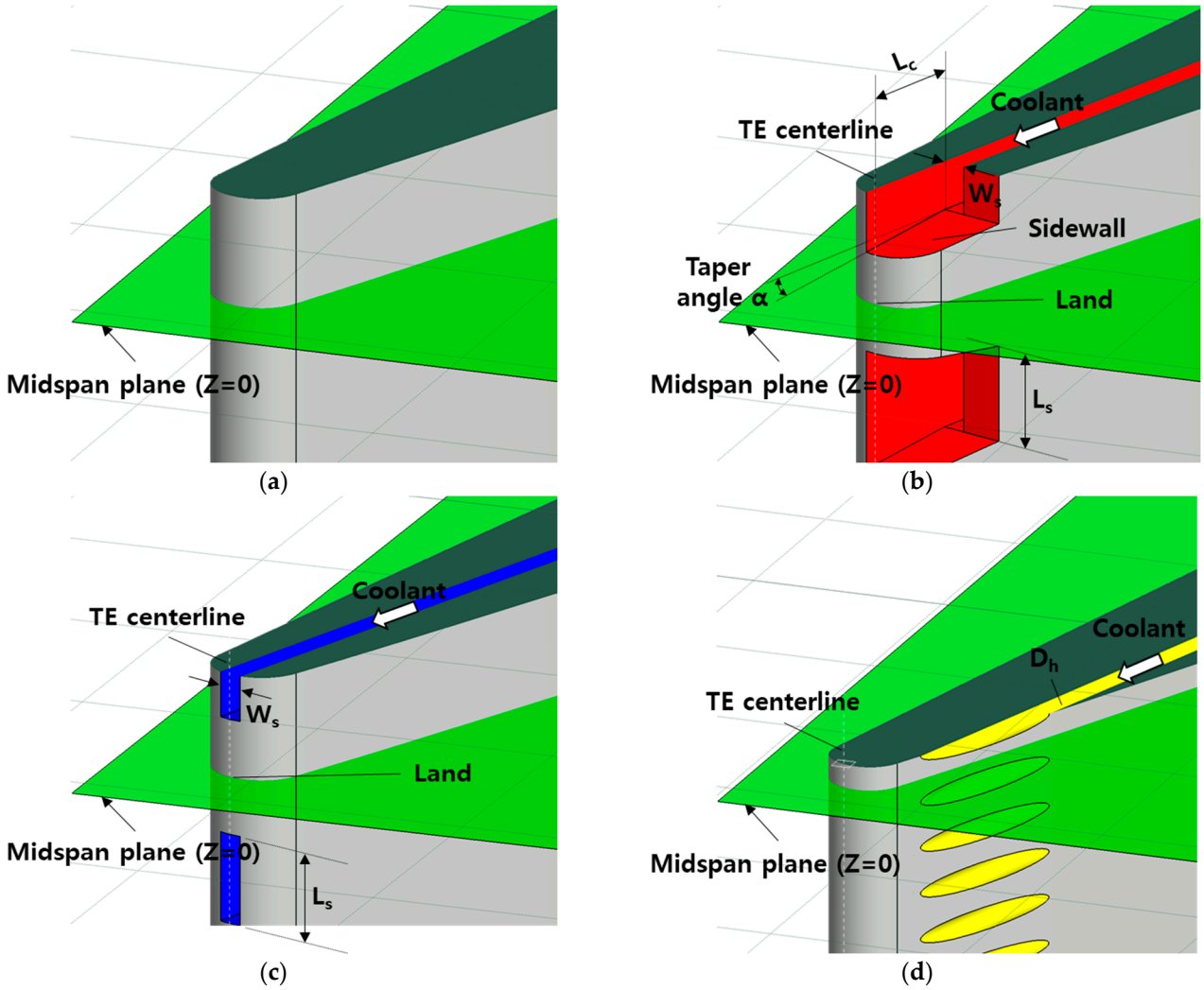

Figure 2. The schematic of the various trailing edge cooling schemes: (**a**) solid(baseline); (**b**) cutback slot; (**c**) central injection slot; (**d**) pressure side hole.

The cutback slot scheme shown in Figure 2b has 8 discrete rectangular slots arranged in a spanwise direction, and the center of the land is located at the midspan height of the vane. The injection angle of the slot is parallel to the vane exit angle. Regardless of the trailing edge diameter, the cutback length L_c and the taper angle α were fixed.

The central injection slot scheme shares the same dimensions as that of the cutback slot, including the hydraulic diameter of the slot, the spacing distance, and the injection angle (Figure 2c). On the other hand, the pressure side hole scheme has 28 discrete cylindrical cooling holes arranged in a spanwise direction (Figure 2d). The diameter of the cylindrical hole corresponds to 75% of the hydraulic diameter of the slot applied to the other schemes, but the total injection area is the same. Therefore, the same amount of coolant is injected through the slot array and the cylindrical hole array for the same blowing ratio conditions. Normalized dimensions of a slot and a cooling hole are presented in Table 1.

Table 1. Cooling scheme design parameters (normalized by the span length H).

Title 1	W_s/H	L_s/H	D_h/H	Number of Cooling Elements
Cutback slot	6.25×10^{-3}	2.5×10^{-2}	N/A	8
Central injection slot	6.25×10^{-3}	2.5×10^{-2}	N/A	8
Pressure side hole	N/A	N/A	7.5×10^{-3}	28

Considering the variations in trailing edge diameters and cooling schemes, a total of 12 vanes were designed and manufactured by using SLA (Stereolithography) type additive manufacturing with 0.1 mm of layer thickness.

The blowing ratio, which means the coolant to the mainstream mass flux ratio, is defined as shown in Equation (1). Four blowing ratios were considered in the present study, i.e., M = 0.0, 1.0, 2.0, and 3.0. And the air was used as the coolant, so the coolant to the mainstream density ratio defined in Equation (2) was 1.0. Here, the mainstream properties were measured at the cascade inlet 150 mm upstream from the leading edge of the vane array.

$$M = \frac{(\rho u)_c}{(\rho u)_\infty} \tag{1}$$

$$DR = \frac{\rho_c}{\rho_\infty} \tag{2}$$

2.3. Linear Cascade

Figure 3 represents the linear cascade for the total pressure loss measurement of the turbine vane. The linear cascade consists of five vanes, which were designed to be replaceable. The vane to be tested was positioned at the center, #3 in Figure 3. Adjacent vanes have an identical trailing edge diameter to that of the tested vane. But the cooling scheme was applied to only the tested vane so that coolant injection did not occur from the adjacent vanes (#1, #2, #4, and #5).

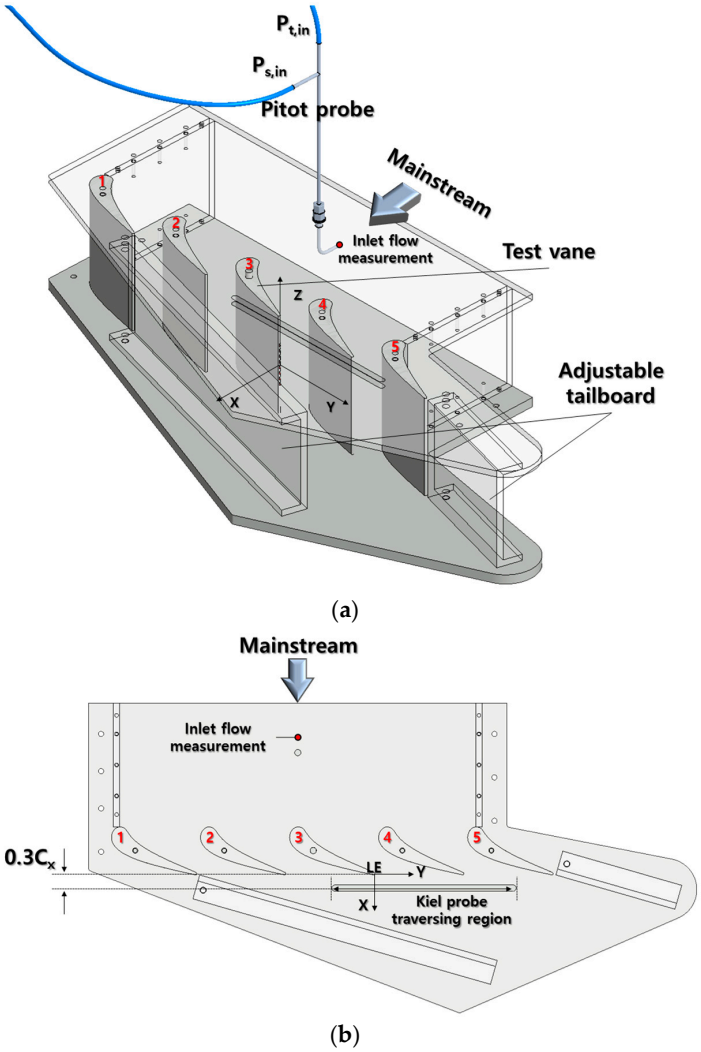

Figure 3. Experimental setup for the total pressure loss measurement: (**a**) 3D view; (**b**) top view.

The total pressure loss measurement was performed at 20 m/s of the mainstream velocity measured using a Pitot probe at the cascade inlet. The inlet flow Reynolds number based on the axial chord length and the mainstream velocity was about 1.64×10^5. The mainstream boundary layer thickness and the turbulence intensity measured using a hot-wire anemometer at the same location of the Pitot probe were about 8 mm and 1.1%, respectively.

At the cascade outlet, a pair of adjustable tailboards was installed to allow the periodic flow of the cascade. In order to confirm the periodicity of the mainstream, the total pressure loss defined in Equation (3) was measured using a 2-axis traverse system with a Kiel probe (KBC-12, United Sensor Corp.) at the midspan height (Z/H = 0) and 0.3 axial chord length downstream from the trailing edge. In Equation (3), subscriptions t and s refer to the total pressure and the static pressure, and in and out indicate the cascade inlet and the outlet, respectively. Figure 4 presents the total pressure loss distribution over 2 pitches of the cascade and shows a good periodic flow field.

$$Cp_t = \frac{\Delta P_t}{(1/2\rho u^2)_{in}} = \frac{P_{t,in} - P_{t,out}}{P_{t,in} - P_{s,in}} \quad (3)$$

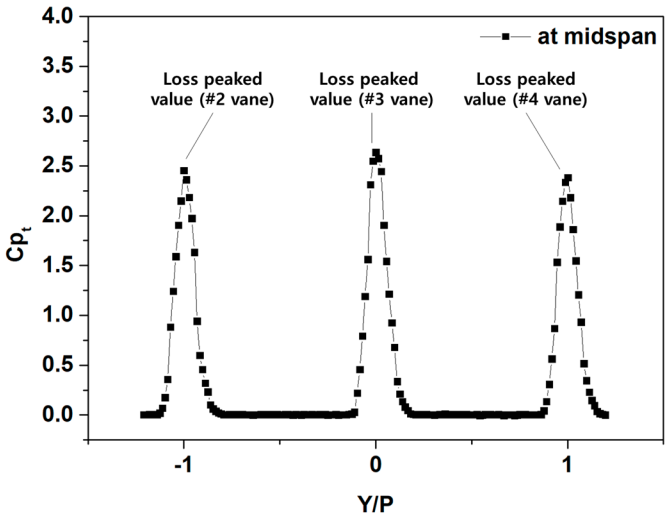

Figure 4. Periodicity of the cascade mainstream.

2.4. Measurement Region of the Total Pressure Loss

In order to evaluate the aerodynamic loss of vane trailing edges with various configurations, the total pressure was measured using a 2-axis traverse and a Kiel probe at the 0.3 axial chord length downstream from the vane trailing edge, as presented in Figure 3b. Figure 5 shows the measurement region for the total pressure loss. In this study, in order to exclude the influence of secondary flow near the endwall, the measurement was focused on the region over the range of Z/H = ±0.1 with respect to the midspan, which is marked in the red dashed box. In addition, the traversing step size on the measurement plane was 1 mm to provide a high resolution of the total pressure loss distribution.

2.5. Measurement Uncertainty Estimation

As defined in Equation (3), the total pressure loss coefficient is a function of pressure terms. The measurement uncertainty was estimated by calculating the propagation of uncertainties. The method used in the study was well-documented by Kline [17]. For the solid vane, the measurement uncertainty was estimated to be ±0.87% at the trailing edge downstream region, i.e., Y/P = 0, in which the total pressure loss coefficient was Cp_t = 2.8.

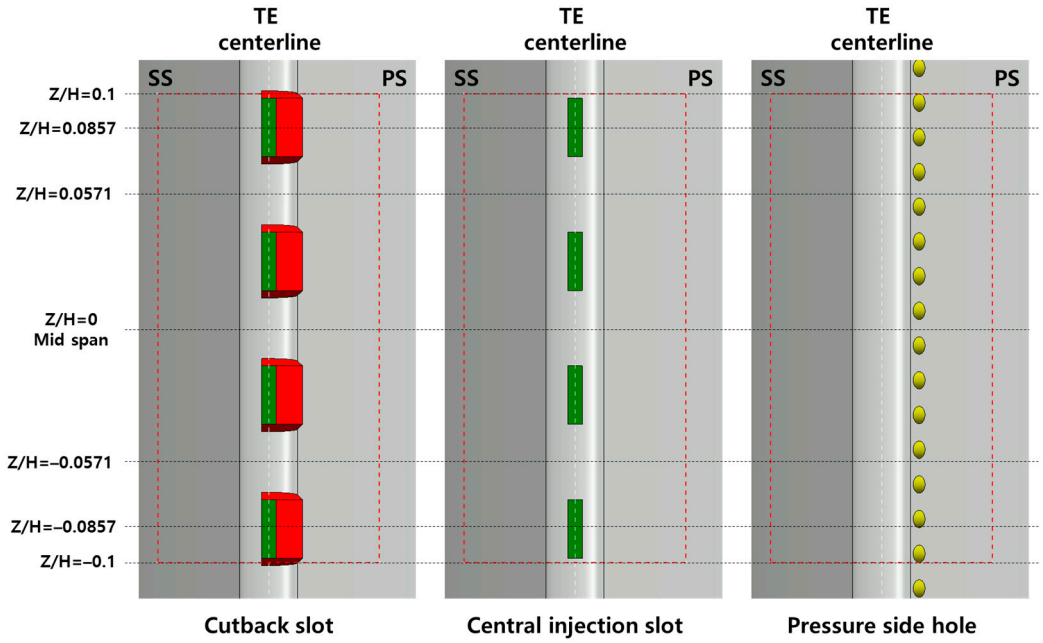

Figure 5. Measurement region of the total pressure loss (rear view).

3. Results

3.1. Comparison of Cooling Schemes

Figure 6 represents the total pressure loss coefficient distribution for various cooling schemes applied to the vane of which the diameter corresponds to 12.5% of the throat width ($d_{TE}/T = 12.5 \times 10^{-2}$). In the case of the solid vane, as shown in Figure 6a, a column-shaped distribution of the total pressure loss was observed, and high values of local pressure loss were distributed in the region of $-0.05 < Y/P < 0$, which corresponds to the downstream of the trailing edge, but the values were gradually diminished as the distance from the core region increased.

Figure 6b–d shows that the distribution of the total pressure loss is strongly affected by the cooling scheme regardless of the blowing ratio condition. For the cutback slot scheme, a sinusoidal wave-like pressure loss distribution was observed on the pressure side in a spanwise direction, and this distribution became more noticeable as the blowing ratio increased, as shown in Figure 6b. In addition, the peaked values of the total pressure loss were observed at locations $Z/H = -0.057$, 0, and 0.057, which correspond to the location of land, and the total pressure loss distribution at the corresponding locations was widely developed in the pressure side direction (positive pitchwise direction). In contrast, narrower distribution of the pressure loss in a pitchwise direction was found at $Z/H = \pm 0.028$ where the center of the slot exit was positioned.

In Figure 6c, the central injection slot scheme shows a similar distribution of the total pressure loss with the solid trailing edge at which the coolant injection was not presented because the airfoils of the two vanes were similar except for the central injection slot on the trailing edge, resulting in a similar flow field behind the trailing edge. However, the deviation between the two cases became larger as the blowing ratio increased, as shown in Figure 6c. At higher blowing ratio conditions, M = 2.0 and M = 3.0, the distribution of the total pressure showed a wavy pattern in the spanwise direction, which is similar to that of the cutback slot scheme.

In the case of the cutback slot, an asymmetric distribution of the total pressure loss was observed in the pitchwise direction regardless of coolant injection. This is because additional flow separations from the lip and cutback surface on the pressure side induced the increase in the total pressure loss.

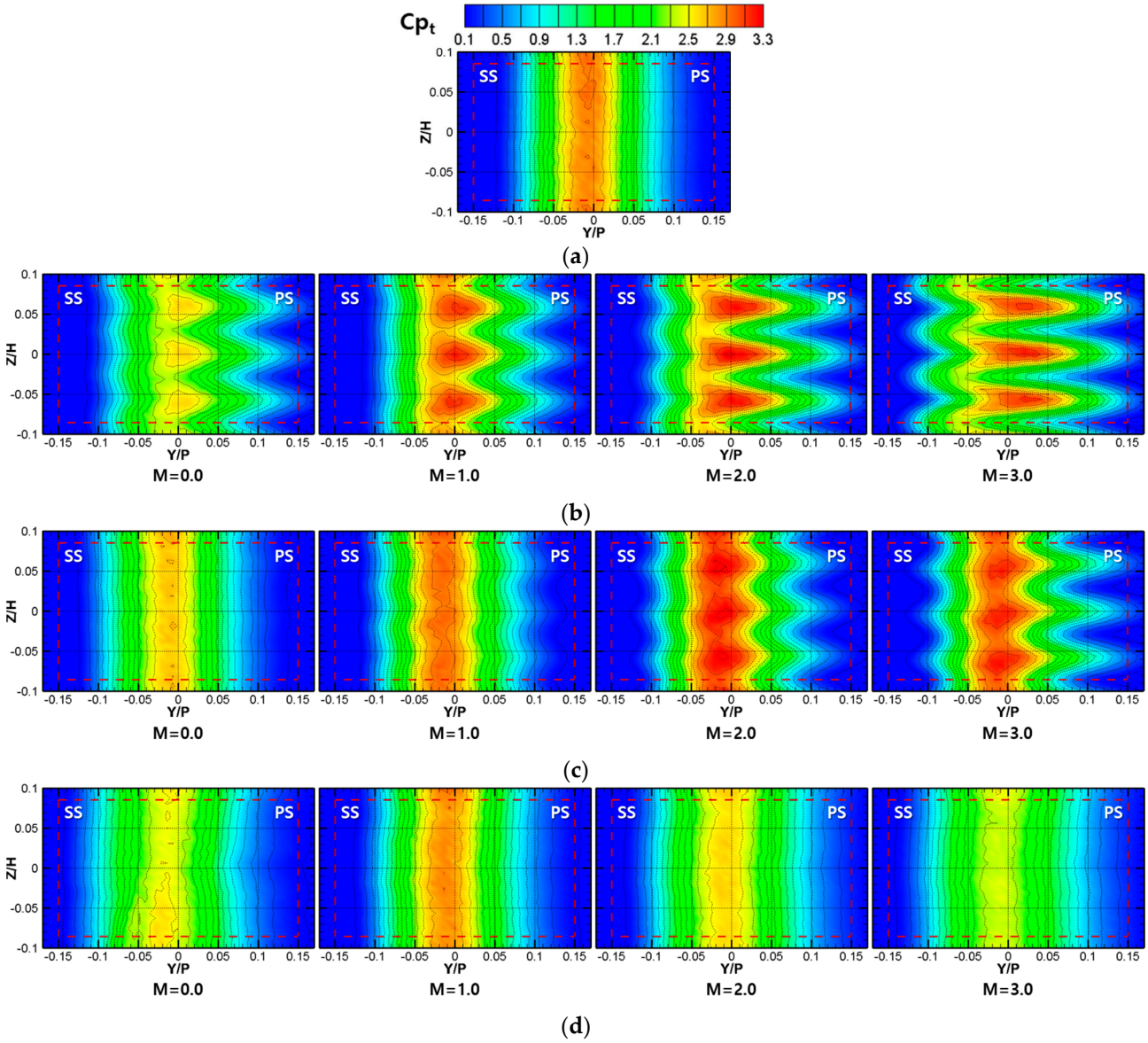

Figure 6. Distribution of the total pressure loss coefficient for various cooling schemes applied to the vane with $d_{TE}/T = 12.5\%$: (**a**) solid; (**b**) cutback slot; (**c**) central injection slot; (**d**) pressure side hole.

In the central injection slot, when the coolant injection was absent, a column shape of the pressure loss distribution, which is symmetrical in the pitchwise direction, was observed, similar to the result of the solid background. This implies that the existence of the central injection slot does not have a significant effect on the total pressure loss when the coolant injection is excluded. On the other hand, when the coolant injection was present, the wake region in the pitchwise direction remained almost constant on the suction side, while the opposite happened on the pressure side. This uneven formation of the wake region is caused by the interaction between the mainstream and the injected coolant. A similar result can be found in work by Aminossadati and Mee [8].

The pressure side hole scheme in Figure 6d shows a similar distribution of the total pressure loss distribution with the solid trailing edge. Unlike the cutback slot scheme, the pressure side hole scheme consists of relatively tiny holes with close spacing. Due to the closely distributed holes, the coolant injected from cooling holes creates a uniform flow field; as a result, the total pressure loss for the pressure side hole scheme is similar to that of the solid vane.

Figure 7 represents the pitchwise distribution of the total pressure loss coefficient at the mid-span height (Z/H = 0). In all cases except for the cutback slot scheme, the pitchwise distribution was nearly symmetrical with respect to Y/P = 0, in which the maximum value was drawn. However, in the case of the cutback slot scheme, the total pressure loss was developed toward the pressure side at the location Z/H = 0, where the center of the land was positioned. As mentioned above, this can be explained by the additional flow separation due to the cutback geometry located on the pressure side and the subsequent growth of the wake.

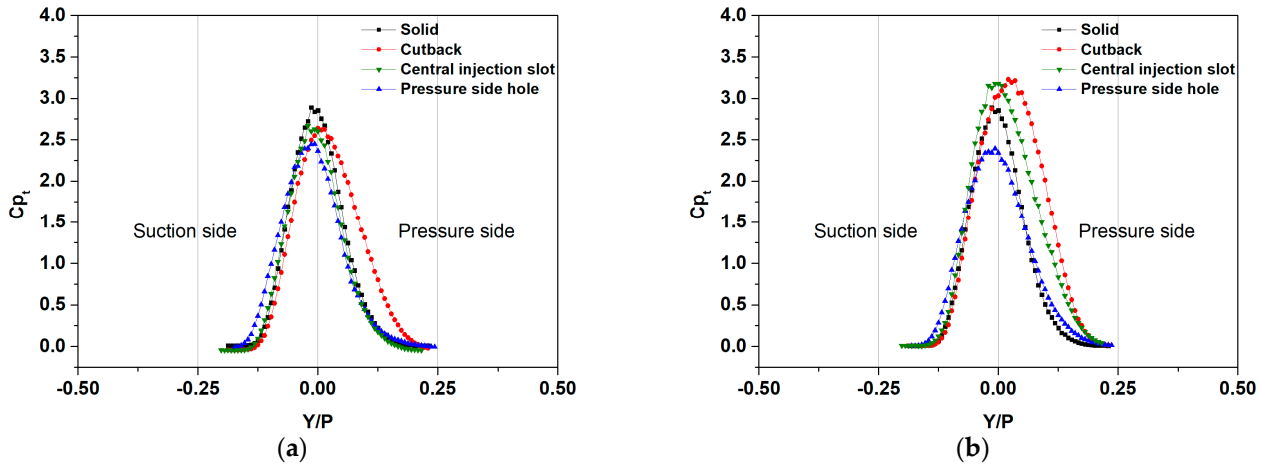

Figure 7. Pitchwise distribution of the total pressure loss coefficient at Z/H = 0: (**a**) for M = 0.0; (**b**) for M = 3.0.

When sufficient coolant is injected, the total pressure loss decreases behind the slot exit (Z/H = ±0.03125), where the momentum of the coolant jet remains high. In contrast, the total pressure loss increased behind the solid land (Z/H = 0, and ±0.057125) where the coolant jet is diffused, and its momentum became weak. So, the total pressure loss in the cases of the cutback slot and the central injection slot increased, as shown in Figure 7b.

3.2. Effect of the Trailing Edge Diameter

Figure 8 shows the distribution of the total pressure loss coefficient when the coolant injection was absent, i.e., M = 0.0 condition. In general, it seemed that the distribution of the total pressure loss became widen as the trailing edge diameter increased regardless of cooling schemes. In the case of the solid vane, the total pressure loss in the region of $-0.04 < Y/P < 0.01$ was developed wider and stronger for larger trailing edge diameters.

The spanwise averaged total pressure loss coefficient was compared in Figure 9. The region marked with a red dashed box represents the region where the average was taken. Regardless of the cooling schemes, as the trailing edge diameter increased, the total pressure loss was found to be more widely distributed, which shows a typical effect of the trailing edge thickness [4]. Particularly, in the case of the cutback slot scheme, a significant increase in the total pressure loss was observed for a bigger trailing edge diameter.

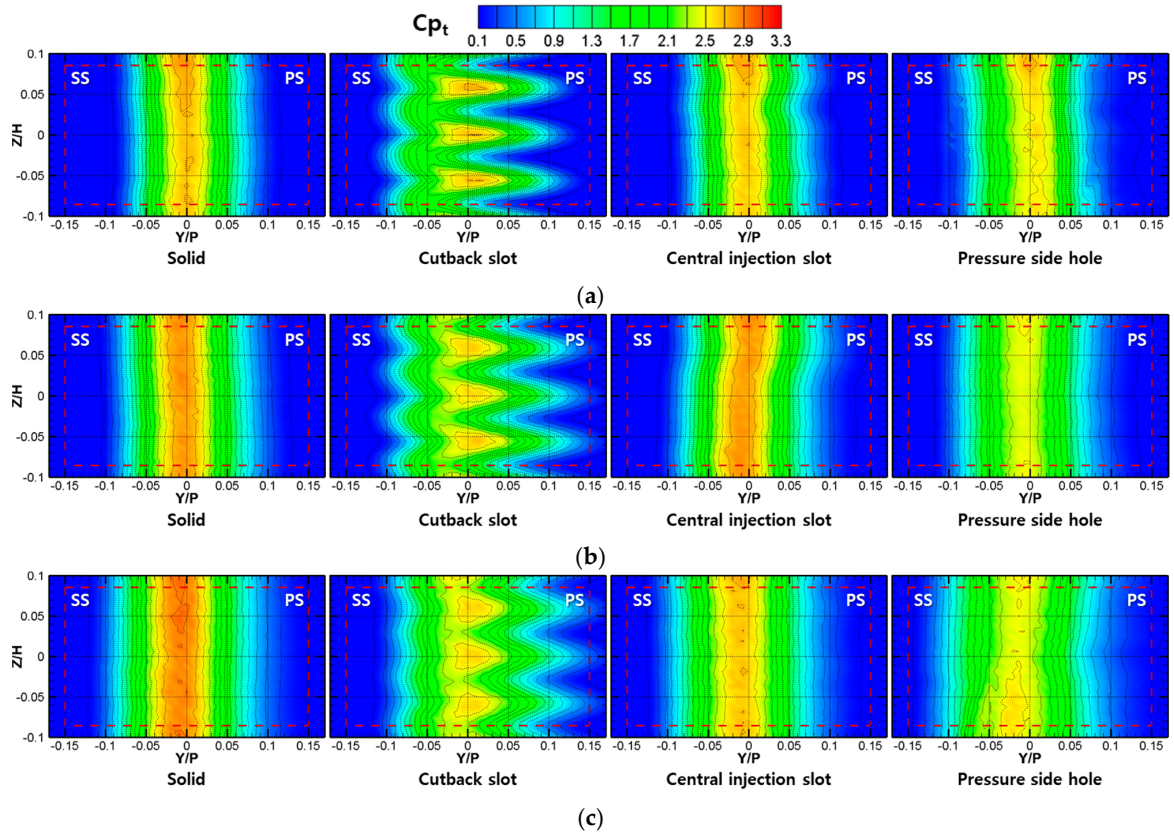

Figure 8. Distribution of the total pressure loss coefficient for different trailing edge diameters at M = 0.0: (**a**) d_{TE}/T = 7.5%; (**b**) d_{TE}/T = 10.0%; (**c**) d_{TE}/T = 12.5%.

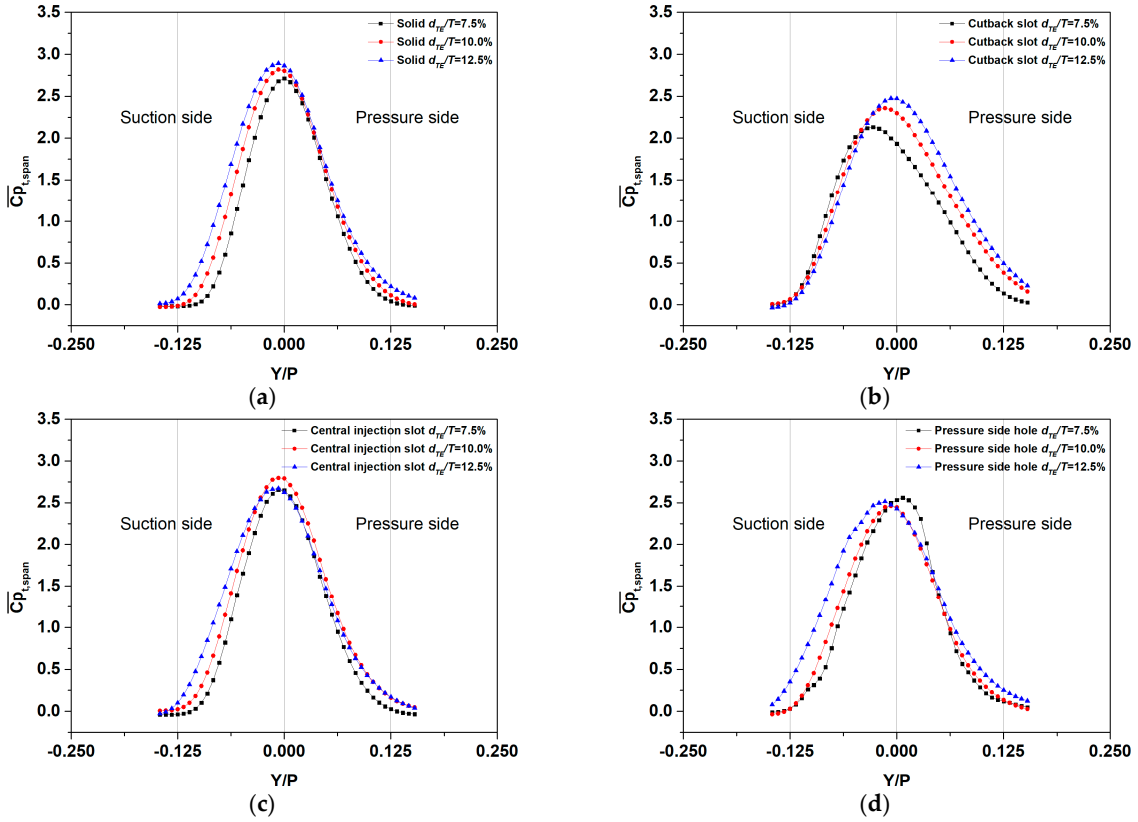

Figure 9. Spanwise averaged total pressure loss coefficient showing the effect of the trailing edge diameter: (**a**) solid; (**b**) cutback slot; (**c**) central injection slot; (**d**) pressure side hole.

3.3. *Effect of the Blowing Ratio*

When the coolant injection is present, mixing occurs due to the difference in momentum between the coolant and the mainstream downstream of vanes (or blades), which causes mixing losses. In other words, the minimum mixing loss can be obtained if the momentum of the coolant is identical to that of the mainstream [6].

Figure 10 represents the distribution of the total pressure loss coefficient for the vane of which the diameter corresponds to 7.5% of the throat width ($d_{TE}/T = 7.5\%$). Specifically, Figure 10a indicates the results at which the coolant injection did not occur. Compared with Figure 10a, the total pressure loss for the coolant injection cases, shown in Figure 10b,c, increased as the blowing ratio increased up to M = 2.0. At that range, the interaction between the mainstream and the coolant with less momentum increased the mixing loss in the wake region.

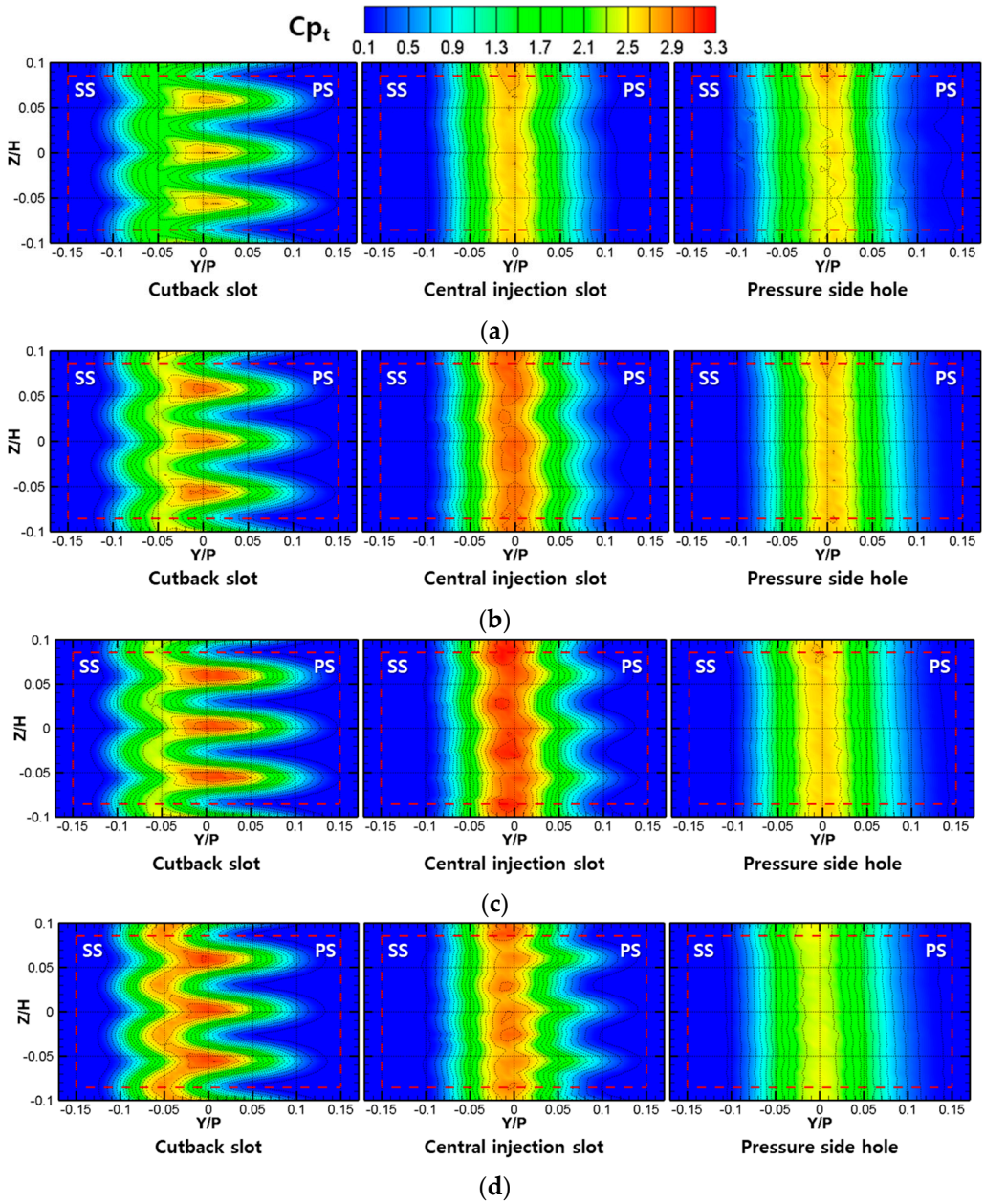

Figure 10. Distribution of the total pressure loss coefficient of the vane trailing edge diameter of $d_{TE}/T = 7.5\%$ at different blowing ratios: (**a**) M = 0.0; (**b**) M = 1.0; (**c**) M = 2.0; (**d**) M = 3.0.

However, this trend was reversed at the condition of the highest blowing ratio, M = 3.0, at which the total pressure loss was smaller than that of M = 2.0. This phenomenon can be attributed to the pressure recovery due to momentum addition by the coolant with sufficiently high momentum when the blowing ratio exceeds a certain level, which was M = 3.0 in this study. A similar trend of the coolant injection was also found in the works by Gao et al. [14] and Rehder [16].

The effect of the blowing ratio can be confirmed through the area-averaged total pressure loss coefficient presented in Figure 11. The area-average was taken across the region marked in a red dashed box Unlike the pressure side hole and the central injection slot schemes, the cutback slot scheme showed that the area-averaged total pressure loss continuously increased as the blowing ratio increased in cases of the vane with $d_{TE}/T = 10.0$ and 12.5%, shown in Figure 11b, c. However, the rate of increase, the slope, of total pressure loss gradually decreased as the blowing ratio increased.

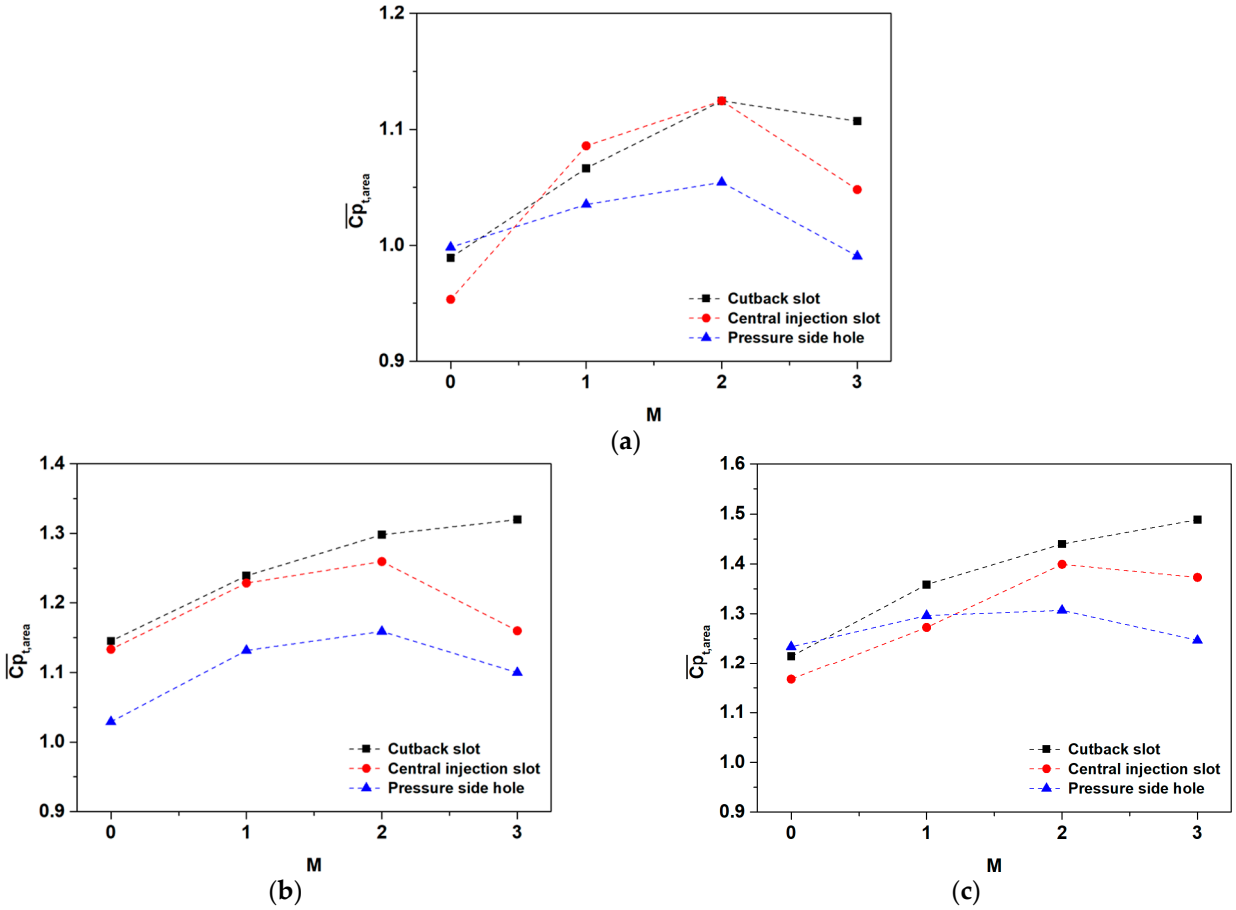

Figure 11. Area averaged total pressure loss coefficient for blowing ratios: (**a**) d_{TE}/T = 7.5%; (**b**) d_{TE}/T = 10.0%; (**c**) d_{TE}/T = 12.5%.

3.4. Correlation Equations

Table 2 presents correlation equations and coefficients for the total pressure loss coefficient. The correlation equations were derived in the form of polynomial equations with a 95% confidence interval. Figure 12 represents the 3D contours of the correlation equations against the trailing edge diameter and the blowing ratio. The coefficient of determination R^2 for each correlation equation exceeded the value of 0.99, which indicates the goodness of fit with the experimental results. Results show that the total pressure loss increased as the trailing edge diameter increased, and for a given trailing edge diameter, the peaks of total pressure loss are observed near the blowing ratio of 2.0.

Table 2. Correlation equations and coefficients.

	$\Lambda = a + bA + cB + dA^2 + eAB + fB^2 + gA^2B + hAB^2 + iB^3$ where, Λ : total pressure loss coefficient A : trailing edge diameter B : blowing ratio				
Cutback slot	a 0.0728	b 0.1679	c 0.1369	d −0.0061	e −0.01407
	f −0.01436	g 0.0012	h -2.50×10^{-5}	i −0.0016	R^2 0.9989
Central injection slot	a −0.5657	b 0.2996	c 0.7842	d −0.01292	e −0.1384
	f −0.01764	g 0.006764	h 0.003849	i −0.01455	R^2 0.9962
Pressure side hole	a 1.73	b −0.1859	c −0.2953	d 0.01167	e 0.07373
	f 0.002852	g −0.00347	h −0.0011	i −0.00531	R^2 0.9966

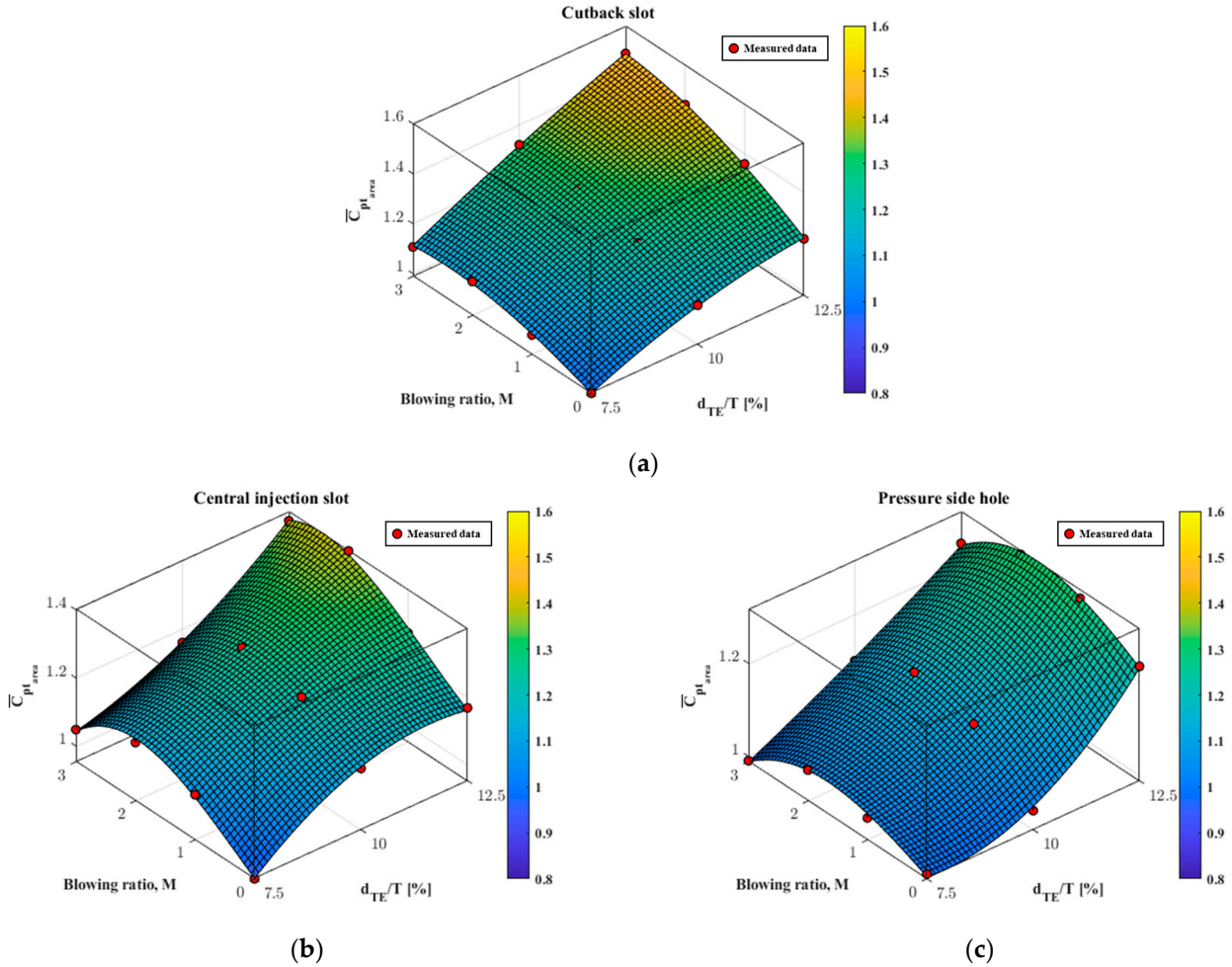

Figure 12. 3D contours of correlation equations for each cooling scheme: (**a**) cutback slot; (**b**) central injection slot; (**c**) pressure side hole.

4. Conclusions

A comparison of the aerodynamic loss of a gas turbine vane with various trailing edge configurations was performed by measuring the total pressure loss downstream of the vane

array. For the trailing edge, three levels of trailing edge diameter (7.5, 10.0, and 12.5% of the throat width) and three different cooling schemes (the cutback slot, the central injection slot, and the pressure side hole) were considered. The correlation equations of the total pressure loss for each cooling scheme were derived against the trailing edge diameter and the blowing ratio. Based on the results, the following conclusions were obtained.

- Different distributions of the total pressure loss were observed for the cooling schemes applied to the vane trailing edge. The cutback slot and the central injection slot schemes showed a periodic wave-like distribution of the total pressure loss in accordance with the arrangement of cooling slots. But the pressure side hole scheme showed a relatively uniform distribution of the total pressure loss;
- Regardless of cooling schemes, it was found that larger trailing edge diameters tend to result in higher total pressure loss of the vane;
- The total pressure loss increased as the blowing ratio increased. However, except for the cutback slot scheme, the total pressure loss rather decreased if the blowing ratio exceeded a certain level (M = 2.0 in this study);
- Correlation equations for each cooling scheme were derived against the trailing edge diameter and the blowing ratio. And they showed a high level of coefficient of determination ($R^2 > 0.99$) and goodness of fit with the experimental results.

In this study, the total pressure loss was measured in a low-speed linear turbine cascade, and a fundamental database set was provided for the aerodynamic design of gas turbine vanes. As a follow-up study, it is recommended to conduct experimental studies in engine-representative mainstream and coolant density ratio conditions.

Author Contributions: Conceptualization, G.-M.K., J.-Y.J., and J.-S.K.; methodology, G.-M.K. and J.-Y.J.; software, Y.-J.K.; validation, J.-Y.J. and Y.-J.K.; formal analysis, G.-M.K.; investigation, G.-M.K., J.-Y.J. and Y.-J.K.; resources, J.-S.K.; data curation, G.-M.K. and J.-Y.J.; writing—original draft preparation, G.-M.K.; writing—review and editing, G.-M.K. and J.-S.K.; visualization, G.-M.K. and J.-Y.J.; supervision, J.-S.K.; project administration, J.-S.K.; funding acquisition, J.-S.K. All authors have read and agreed to the published version of the manuscript.

Funding: This research was supported by Basic Science Research Program through the National Research Foundation of Korea (NRF), funded by the Ministry of Education (Grant No. 2022R1A6A1A03056784).

Data Availability Statement: Data sharing is not applicable to this article.

Conflicts of Interest: The authors declare no conflict of interest.

Nomenclature

C	chord length (mm)
C_{pt}	total pressure loss coefficient
Cx	axial chord length (mm)
DR	density ratio (ρ_c/ρ_∞)
d_{TE}	trailing edge diameter(mm)
H	span height (mm)
L_c	cutback length (mm)
L_s	cutback slot height (mm)
M	blowing ratio $(\rho u)_c/(\rho u)_\infty$
P	pressure (Pa)
u	velocity (m/s)
W_s	cutback slot width (mm)
X	streamwise coordinate which parallels the cascade mainstream (mm)
Y	pitchwise coordinate (mm)
Z	spanwise coordinate with respect to midspan height (mm)

Greek symbols	
α	cutback taper angle (degree)
A	identifier of normalized trailing edge diameter (d_{TE}/T) in correlation equations
B	identifier of blowing ratio (M) in correlation equations
Λ	identifier of the total pressure loss coefficient (C_{pt}) in correlation equations
ρ	density (kg/m^3)
Subscripts	
area	area-averaged value
in	cascade inlet
s	static
span	spanwise averaged value
t	total
TE	trailing edge
out	cascade outlet
∞	mainstream
Abbreviation	
LE	leading edge
PS	pressure side
SS	suction side
TE	trailing edge

References

1. Denton, J.D. Loss Mechanism in Turbomachines. *J. Turbomach.* **1993**, *115*, 621–656. [CrossRef]
2. Mee, D.J.; Baines, N.C.; Oldfield, M.L.G.; Dickens, T.E. An Experimental of the Contributions to Loss on a Transonic Turbine Blade in Cascade. *J. Turbomach.* **1992**, *114*, 155–162. [CrossRef]
3. Melzer, A.P.; Pullan, G. The Role of Vortex Shedding in the Trailing Edge Loss of Transonic Turbine Blade. *J. Turbomach.* **2019**, *141*, 041001. [CrossRef]
4. Granovskiy, A.; Gribin, V.; Lomakin, N. Experimental and Numerical Study of Transonic Cooled Turbine Blades. *Int. J. Turbomach. Propuls. Power* **2018**, *3*, 16. [CrossRef]
5. Parra, J.; Cadrecha, D.; González, E.; Lázaro, B. Trailing Edge Thickness Impact on the Profile Losses of Highly Loaded Low Pressure Turbines Blades. In *Proceedings of the ASME Turbo Expo 2016: Turbomachinery Technical Conference and Exposition, Volume 2B: Turbomachinery, Seoul, Republic of Korea, 13–17 June 2016*; ASME Paper No. GT2016-57955; ASME: New York, NY, USA, 2016.
6. Schobeiri, T. Optimum Trailing Edge Ejection for Cooled Gas Turbine Blades. *J. Turbomach.* **1989**, *111*, 510–514. [CrossRef]
7. Schobeiri, M.T.; Pappu, K. Optimization of Trailing Edge Ejection Mixing Losses: A Theoretical and Experimental Study. *J. Fluids Eng.* **1999**, *121*, 118–125. [CrossRef]
8. Aminossadati, S.M.; Mee, D.J. An Experimental Study on Aerodynamic Performance of Turbine Nozzle Guide Vanes With Trailing-Edge Span-Wise Ejection. *J. Turbomach.* **2013**, *135*, 031002. [CrossRef]
9. Martini, P.; Schulz, A.; Bauer, H.-J. Film Cooling Effectiveness and Heat Transfer on the Trailing Edge Cutback of Gas Turbine Airfoils With Various Internal Cooling Designs. *J. Turbomach.* **2006**, *128*, 196–205. [CrossRef]
10. Martini, P.; Schulz, A.; Bauer, H.-J.; Whitney, C.F. Detached Eddy Simulation of Film Cooling Performance on the Trailing Edge Cutback of Gas Turbine Airfoils. *J. Turbomach.* **2006**, *128*, 292–299. [CrossRef]
11. Holloway, D.S.; Leylek, J.H.; Buck, F.A. Pressure-Side Bleed Film Cooling: Part I—Steady Framework for Experimental and Computational Results. In *Proceedings of the ASME Turbo Expo 2002: Power for Land, Sea, and Air, Volume 3: Turbo Expo 2002, Parts A and B, Amsterdam, The Netherlands, 3–6 June 2002*; ASME Paper No. GT2002-30471; ASME: New York, NY, USA, 2002.
12. Uzol, O.; Camci, C.; Glezer, B. Aerodynamic Loss Characteristics of a Turbine Blade with Trailing Edge Coolant Ejection: Part 1—Effect of Cut-Back Length, Spanwise Rib Spacing, Free-Stream Reynolds Number, and Chordwise Rib Length on Discharge Coefficients. *J. Turbomach.* **2001**, *123*, 238–248. [CrossRef]
13. Uzol, O.; Camci, C. Aerodynamic Loss Characteristics of a Turbine Blade With Trailing Edge Coolant Ejection: Part 2—External Aerodynamics, Total Pressure Losses, and Predictions. *J. Turbomach.* **2001**, *123*, 249–257. [CrossRef]
14. Gao, J.; Wang, F.; Fu, W.; Zheng, Q.; Yue, G.; Dong, P. Experimental Investigation of Aerodynamic Performance of a Turbine Cascade with Trailing-Edge Injection. *J. Aerosp. Eng.* **2017**, *30*, 04017074. [CrossRef]
15. Kaptejin, C.; Amecke, J.; Michelassi, V. Aerodynamic Performance of a Transonic Turbine Guide Vane With Trailing Edge Coolant Ejection: Part I—Experimental Approach. *J. Turbomach.* **1996**, *118*, 519–528. [CrossRef]

16. Rehder, H.J. Investigation of Trailing Edge Cooling Concepts in a High Pressure Turbine Cascade—Aerodynamic Experiments and Loss Analysis. *J. Turbomach.* **2012**, *134*, 051029. [CrossRef]
17. Kline, S.J. The Purpose of Uncertainty Analysis. *J. Turbomach.* **1985**, *107*, 153–160. [CrossRef]